

**CD4⁺ tumor-infiltrating lymphocytes secreting T cell-engagers induce
regression of autologous patient-derived non-small cell lung cancer
xenografts**

Anaïs Jiménez-Reinoso*, Magdalena Molero-Abraham, Cristina Cirauqui, Belén Blanco,
Eva M. Garrido-Martin, Daniel Nehme-Álvarez, Carmen Domínguez-Alonso, Ángel
Ramírez-Fernández, Laura Díez-Alonso, Ángel Nuñez-Buiza, África González-Murillo,
Raquel Tobes, Eduardo Pareja, Manuel Ramírez-Orellana, José L. Rodríguez-Peralto,
Irene Ferrer, Jon Zugazagoitia, Luis Paz-Ares, Luis Álvarez-Vallina*

*Corresponding authors: a.jimenez.imas12@h12o.es, lalvarezv@ext.cnio.es

This Inventory includes:

- **List of Abbreviations**
- **Supplementary Figures**
- **Supplementary Tables**

LIST OF ABBREVIATIONS

ACT: Adoptive cell therapy

CM: central memory

CR: complete responses

DCM: DMEM complete medium

DN: double negative

DP: double positive

DSP: digital spatial profiling

E:T: Effector:target ratio

EBV: Epstein-Barr virus

EGFP: Enhanced green fluorescent protein

EGFR LiTE: anti-EGFR x anti-CD3 light T cell engager

EGFR: epidermal growth factor receptor

ELISA: enzyme-linked immunosorbent assays

EM: effector memory

EMRA: effector memory re-expressing CD45RA

FC: fold change

FDR: false discovery rate

FFPE: formalin-fixed and paraffin-embedded

GZMB: granzyme B

H/E: hematoxylin and eosin.

hIL-2 NOG mice: NOD.Cg-*Prkdc*^{scid} *Il2rg*^{tm1Sug} Tg(CMV-IL2)4-2Jic/JicTac

IHC: immunohistochemistry

IL-2: Interleukin-2

KO: knock out

M: mouse.

NGS: next-generation sequencing

NRTs: neoantigen reactive T cells

NSCLC: non-small cell lung cancer

NTd: Non-transduced

P1: Patient 1

P2: Patient 2

PDX: Patient-derived xenograft

RCM: RPMI complete medium

REP: rapid expansion protocol.

rhIL-2: recombinant human IL-2

ROI: regions of interest

scFv: single-chain variable fragment

SD: standard deviation

SEM: standard error of mean

STAb: Secreting T cell-engaging antibodies

TAA: tumor-associated antigen

TCE: T cell-engagers

TCR: T cell receptor

TME: tumor microenvironment

TIL: tumor-infiltrating lymphocytes

Veh.: vehicle

SUPPLEMENTARY FIGURES

Supplementary Figure S1

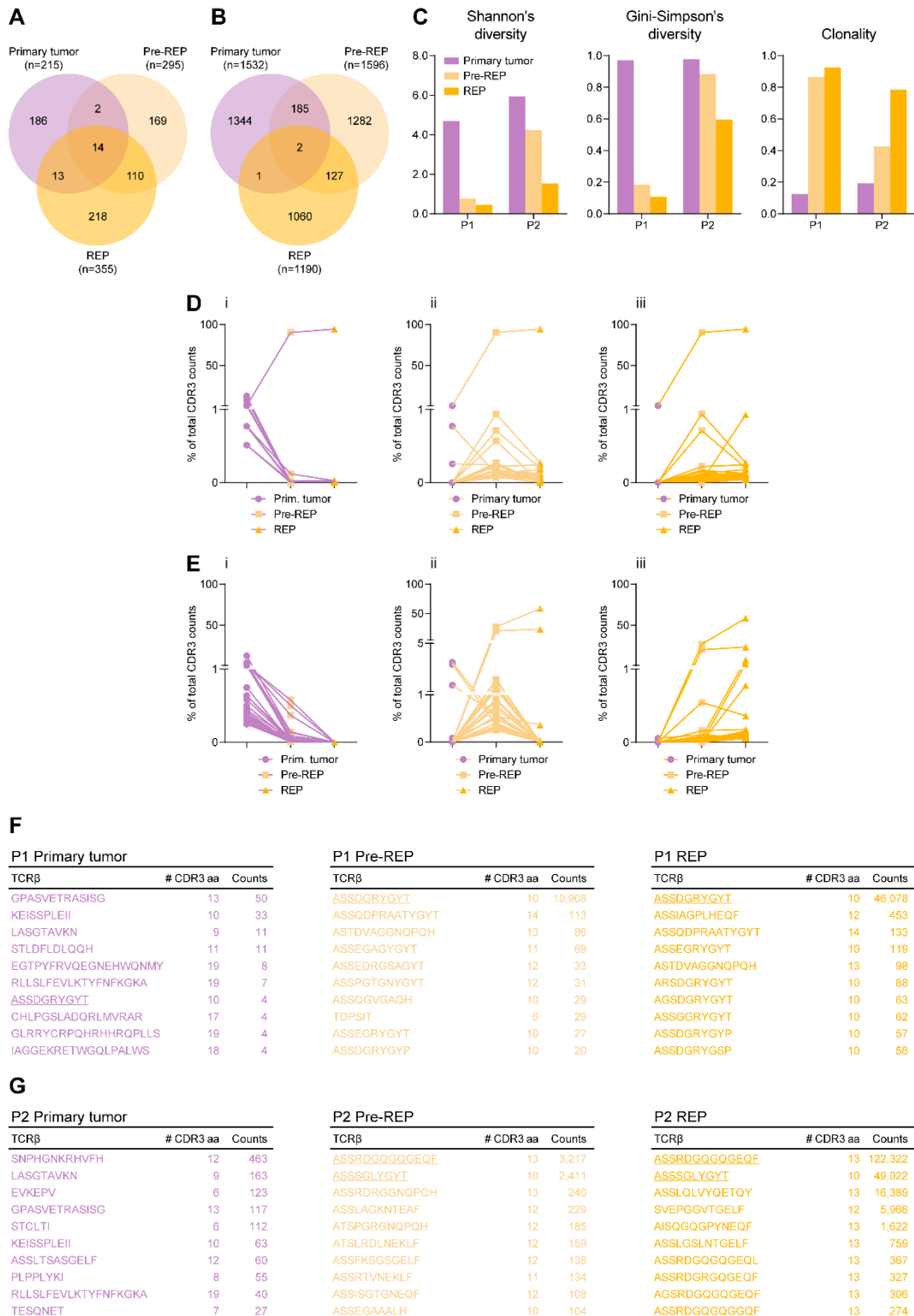


Figure S1. TCRβ clonotypes metrics and clonal dynamics during *ex vivo* TIL expansion. (A, B) Shared clonotypes between primary tumors, pre- and post-REP TIL cultures from NSCLC P1 (A) and P2 (B). (C) NSCLC P1 and P2 TCR Shannon's and Gini-Simpson's diversity scores, and TCR clonality scores in primary tumors and in pre-

and post-REP TIL cultures, calculated from total number of productive clonotypes with amino acid-length between 5-20. **(D, E)** Relative frequency of the TOP-30 largest clones of the primary tumor (i), the pre-REP (ii) or the post-REP (iii) CDR3 repertoire of samples from NSCLC P1 **(D)** and P2 **(E)**. **(F, G)** Detailed amino acid sequences of the TOP-10 largest clones of the primary tumor, the Pre-REP or the Post-REP CDR3 repertoire of samples from NSCLC P1 **(F)** and P2 **(G)**. P1, Patient 1; P2, Patient 2; REP, rapid expansion protocol.

Supplementary Figure S2

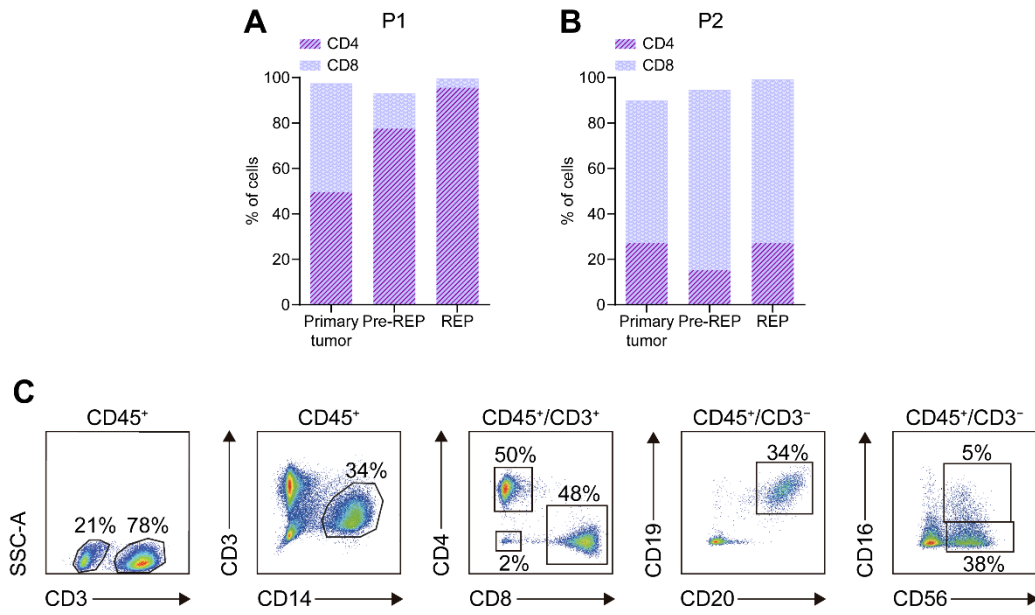


Figure S2. Immune microenvironment phenotype in NSCLC patients. (A, B) Percentages of CD4⁺ and CD8⁺ T cells from NSCLC P1 (A) and P2 (B). (C) Percentages of total T (CD3⁺), non-T (CD3⁻), macrophages (CD3⁻CD14⁺), CD4⁺ and CD8⁺ T cells, B cells (CD19⁺CD20⁺) and NK cells (CD56⁺CD16^{+/-}) within leukocytes (CD45⁺) after P1 primary tumor disaggregation.

Supplementary Figure S3

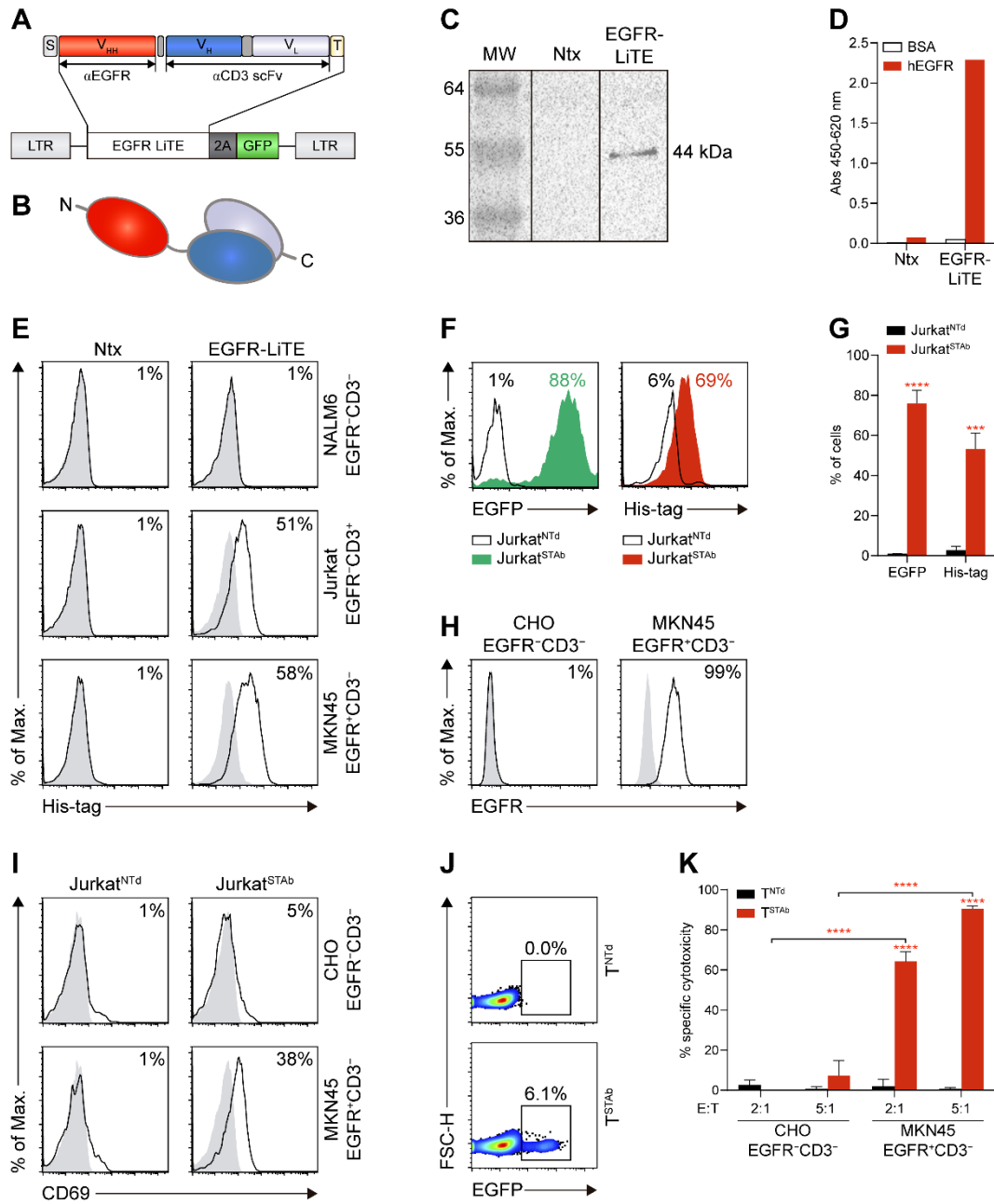


Figure S3. Functionality of secreted anti-EGFR light T cell engagers (LiTE). (A, B) Schematic diagrams showing the genetic (A) and domain structure (B) of the anti-EGFR x anti-CD3 Light T cell engager (EGFR LiTE) bearing the OncoM signal peptide (S, grey box), the anti-EGFR V_{HH} gene (red box), the anti-CD3 scFv gene (blue boxes), and the Myc and His tags (light yellow box). The EGFR LiTE construct was cloned into a pCCL lentiviral-based backbone containing a T2A-EGFP cassette (A). (C, D) Detection of soluble secreted EGFR LiTE in the conditioned media from pCCL transfected HEK293T cells by Western blot (C) or ELISA (D). Conditioned media from non-transfected (NTx) cells was used as negative control. One representative experiment is shown. (E) Binding assays of conditioned media from NTx- or EGFR LiTE-transfected HEK293T cells to NALM6, Jurkat and MKN45 tumor cells. Specific binding was detected using anti-His-tag mAb and analyzed by flow cytometry. (F) Percentage of EGFP-positive (left) and

EGFR-LiTE decorated (right) engineered EGFR-STAb Jurkat (Jurkat^{STAb}) in comparison with non-transduced Jurkat cells (Jurkat^{NTd}). EGFR-LiTE decoration was detected using anti-His-tag mAb and analyzed by flow cytometry. **(G)** EGFP expression and EGFR-LiTE decoration analysis in Jurkat^{NTd} and Jurkat^{STAb} cells. Data represent mean+SEM of at least 3 independent experiments, and statistical significance was calculated by two-way ANOVA test corrected by Sidak's multiple comparisons test; **p < 0.01; ***p < 0.001. **(H)** Cell surface expression profile of EGFR from target cells used in *in vitro* studies by flow cytometry. **(I)** T cell activation assay. Jurkat^{NTd} or Jurkat^{STAb} cells were co-cultured at a 1:1 E:T ratio with EGFR-negative (CHO) or EGFR-positive (MKN45) cells for 24 hours and CD69 expression analyzed by flow cytometry. **(J)** Percentage of EGFP-positive transduced primary T cells (T^{STAb}) in comparison with non-transduced primary T cells (T^{NTd}). **(K)** Specific cytotoxicity of T^{NTd} or T^{STAb} cells against EGFR-negative (CHO) or EGFR-positive (MKN45) cells at the indicated E:T ratios after 48 hours. The percentage of specific cytotoxicity was calculated by adding D-luciferin to detect bioluminescence. Data represent mean+SD and statistical significance was calculated by two-way ANOVA test corrected by Tukey's multiple comparisons test; ****p < 0.0001. The inset numbers in **(E-J)** represent the percentage of cells staining positive for the indicated marker. EGFP, enhanced green fluorescence protein; SEM, standard error of the mean; SD, standard deviation.

Supplementary Figure S4

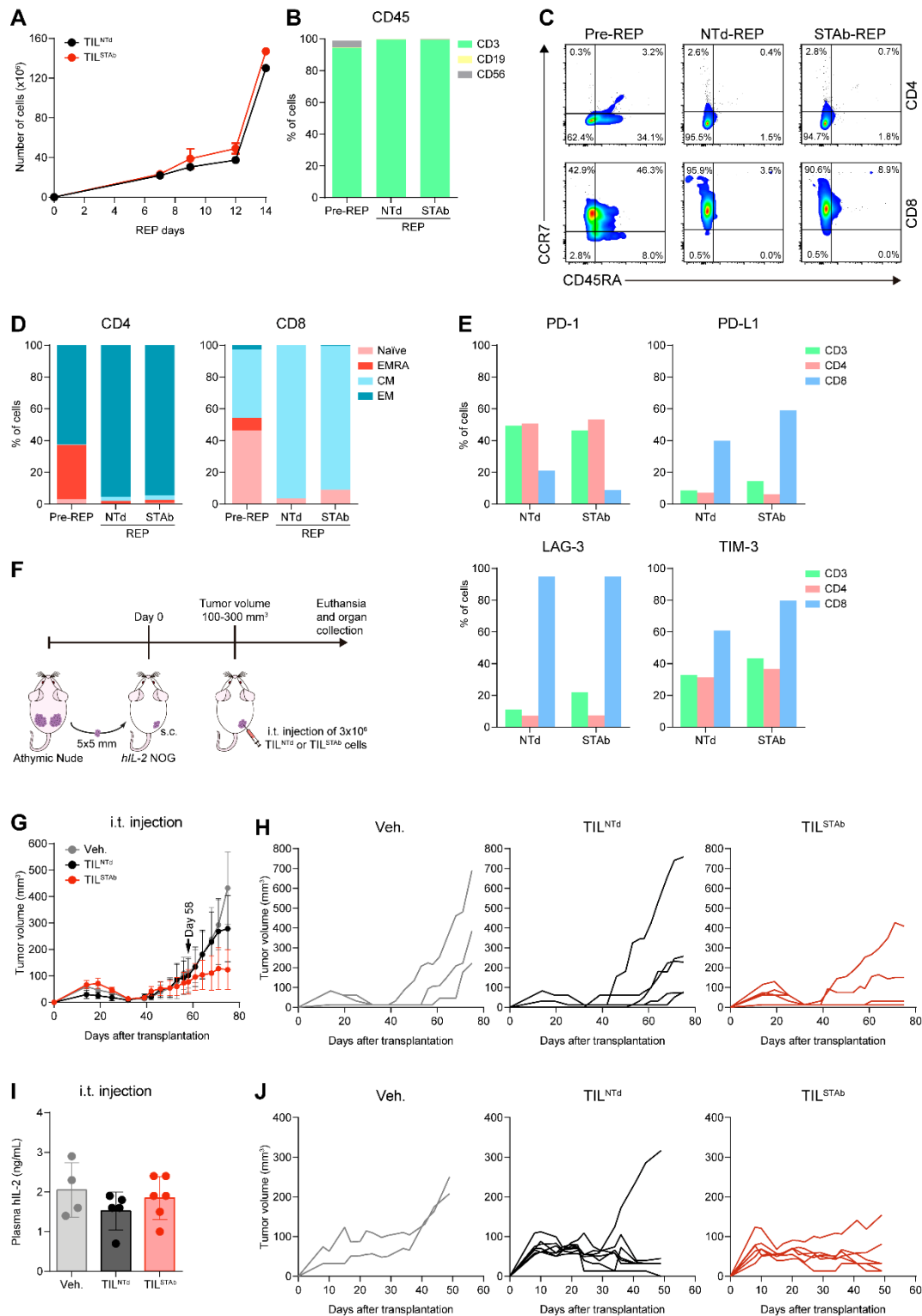


Figure S4. Treatment of EGFR⁺ NSCLC PDX mouse model with autologous engineered TCE-secreting TIL (cont.). (A) Cell growth during the small-scale REP of non-transduced (TIL^{NTd}) and EGFR-STAb TIL (TIL^{STAb}). **(B)** Percentages of total T (CD45⁺CD3⁺), B (CD45⁺CD19⁺) and NK (CD45⁺CD56⁺) cells among Pre-REP TIL, TIL^{NTd} REP and TIL^{STAb} REP. **(C, D)** Plots **(C)** and graph bars **(D)** representing the percentages of naive, effector memory re-expressing CD45RA (EMRA), central memory

(CM), and effector (EM) CD4⁺ or CD8⁺ T cells among pre-REP, TIL^{NTd} REP, and TIL^{STAb} REP. (E) Exhaustion markers expression within total T, CD4 (CD3⁺CD4⁺) and CD8 (CD3⁺CD8⁺) cells after REP. (F) Experimental design of autologous PDX establishment. *hIL-2* NOG xenografted mice were intratumorally (i.t.) treated with 3×10⁶ TIL^{NTd} or TIL^{STAb} cells when the average tumor volume reached approximately 100-300 mm³. After tumors reached the indicated size, thirteen mice were randomized into three groups (3/5/5) and i.t. treated with Veh. (PBS supplemented with 300 IU/mL rhIL-2, *n*=3 mice), TIL^{NTd} (*n*=5 mice) or TIL^{STAb} (*n*=5 mice) cells. Black arrow indicates the day of the injection. Tumors sizes were measured with calipers. (G, H) Tumor growth curves represented as mean±SEM (G) or as individual mouse curves within the different groups (H); black arrow indicates the day of the i.t. injection. (I) Human IL-2 plasma levels in mice after TIL treatment (mean±SD). Significance was calculated by two-way (G) or one-way (I) ANOVA test corrected by Tukey's multiple comparisons test; no significant differences were found. (J) Tumor growth curves represented as individual mouse curves within the different groups of *hIL-2* NOG xenografted mice intravenously (i.v.) treated with 7.5×10⁶ TIL^{NTd} or TIL^{STAb} cells when the average tumor volume reached approximately 100-300 mm³. Veh., vehicle; SEM, standard error of mean; SD, standard deviation.

Supplementary Figure S5

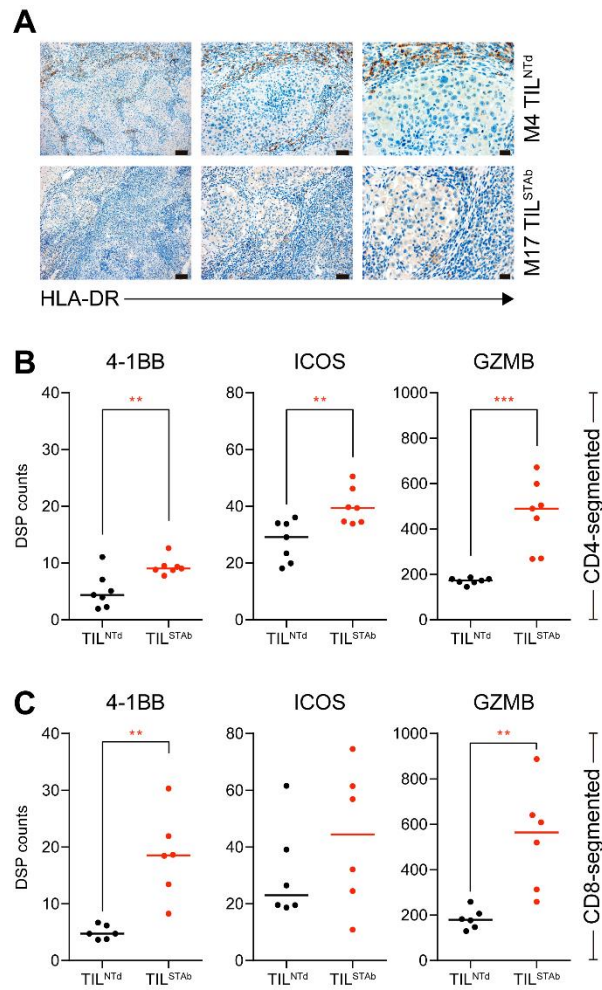


Figure S5. Immunohistochemistry and DSP analysis of intravenously treated *hIL2* xenografted mouse 4 (TIL^{NTd}-treated) and mouse 17 (TIL^{STAb}-treated) (cont.). (A) Expression of HLA-DR after treatment of *hIL2* NOG xenografted mouse 4 (M4) with TIL^{NTd} or mouse 17 (M17) with TIL^{STAb}. Scale bars: 100 μ m (left), 50 μ m (middle) and 20 μ m (right). (B) Comparative analysis of 4-1BB, ICOS, and GZMB levels measured by DSP in CD4 (B) or CD8 (C) compartments. Significance was calculated by an unpaired t-test. **p < 0.01; ***p < 0.001. GZMB, granzyme B.

Supplementary Figure S6

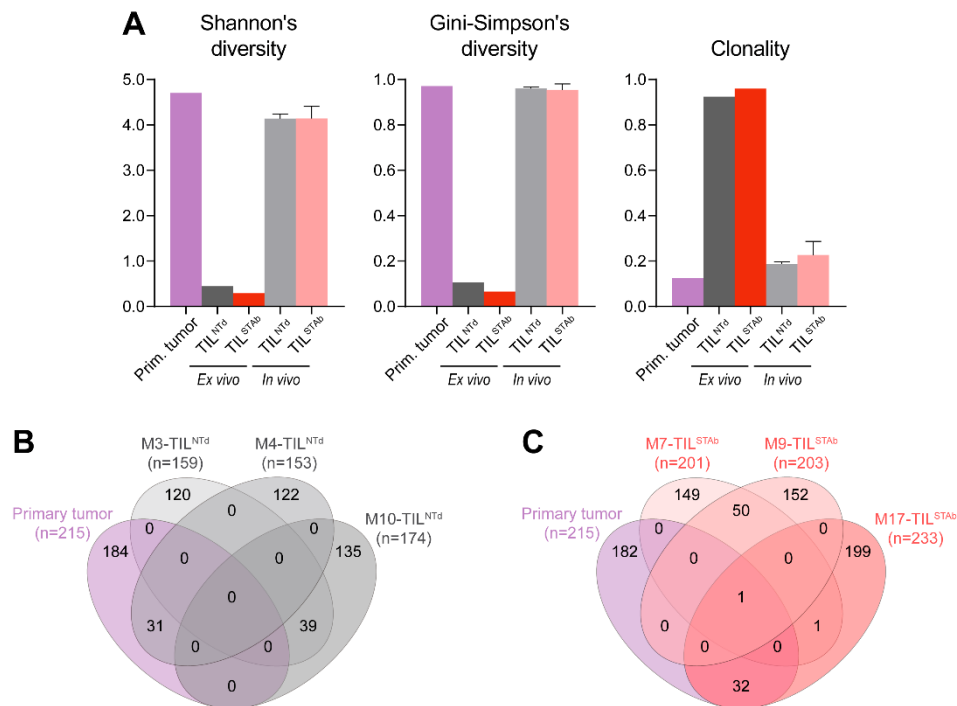


Figure S6. TCR clonotypes composition of primary tumor and *in vivo* TIL-treated tumors from NSCLC P1. (A) Shannon's and Gini-Simpson's diversity scores, and TCR clonality scores in primary tumor (Prim. Tumor), *ex vivo* expanded TIL and *in vivo* TIL-treated tumors. (B, C) Shared clonotypes between primary tumor and *in vivo* TIL^{NTd}-treated (B) or TIL^{STAb}-treated tumors (C). Data in (A-C) are calculated from total number of unique productive clonotypes with 5-20 amino acid length CDR3 of TCR β .

SUPPLEMENTARY TABLES

Table S1. Antibodies

Antigen	Clone	Host species / clonality	Brand	Reference	Application
Anti-GFP	D5.1	Rabbit monoclonal	Cell Signaling Technology	2956	IHC
Anti-human CD3	LN10	Mouse monoclonal	Leica	CD3-565-L-CE	IHC
Anti-human CD3 FLEX-X	–	Rabbit Polyclonal	Dako	IR503	IHC
Anti-human CD4	4B12	Mouse monoclonal	Leica	CD4-368-L-CE	IHC
Anti-human CD8	4B11	Mouse monoclonal	Leica	CD8-4B11-L-CE	IHC
Anti-human CD31	JC70A	Mouse monoclonal	Leica	CD31-607-L-CE	IHC
Anti-human CD31	EPR17259	Rabbit monoclonal	Abcam	ab182981	IHC
Anti-human EGFR	H11	Mouse monoclonal	Dako	M3563	IHC
Anti-human HLA-DR, α -chain	TAL.1B5	Mouse monoclonal	Dako	M0746	IHC
Anti-human Perforin	5B10	Mouse monoclonal	Invitrogen	MA512469	IHC
Anti-human FOXP3	236A/E7	Mouse monoclonal	eBioscience	14-4777-82	IHC
Anti-His APC	GG11-8F3.5.1	Mouse monoclonal	Miltenyi Biotec	130-119-782	FC
Anti-human CD3 V450	UCHT1	Mouse monoclonal	BD Horizon	560365	FC
Anti-human CD3 FITC	HIT3a	Mouse monoclonal	BD Pharmingen	561802	FC
Anti-human CD4 BUV395	RPA-T4	Mouse monoclonal	BD Horizon	564724	FC
Anti-human CD4 PerCP-Cy5.5	SK3	Mouse monoclonal	BD	332772	FC
Anti-human CD8 BUV563	RPA-T8	Mouse monoclonal	BD Horizon	565695	FC
Anti-human CD8 APC-Cy7	SK1	Mouse monoclonal	BioLegend	344714	FC
Anti-human CD14 BV605	M5E2	Mouse monoclonal	BD Horizon	564054	FC

Anti-human CD16 Brilliant Violet 785™	3G8	Mouse monoclonal	Biolegend	302045	FC
Anti-human CD19 PE- Cy7	HIB19	Mouse monoclonal	eBioscience™	25-0199-42	FC
Anti-human CD19 APC	HIB19	Mouse monoclonal	BD Pharmingen	555415	FC
Anti-human CD20 APC	2H7	Mouse monoclonal	BioLegend	302309	FC
Anti-human CD25 FITC	M-A251	Mouse monoclonal	BD Pharmingen	555431	FC
Anti-human CD45 V500-C	2D1	Mouse monoclonal	BD Horizon	655873	FC
Anti-human CD45 Alexa Fluor® 700	HI30	Mouse monoclonal	BD Pharmingen	560566	FC
Anti-human CD45RA V500	HI100	Mouse monoclonal	BD Horizon	561640	FC
Anti-human CD56 PE- Cy7	NCAM16.2	Mouse monoclonal	BD	335826	FC
Anti-human CD56 APC	B159	Mouse monoclonal	BD Horizon	555518	FC
Anti-human CCR7 BV421	150503	Mouse monoclonal	BD Horizon	562555	FC
Anti-human EGFR	EGFR.1	Mouse monoclonal	BD Horizon	566254	FC
Anti-human HLA-DR PE-Cy7	G46-6	Mouse monoclonal	BD Pharmingen	560651	FC
Anti-human TCRg/d FITC	11F2	Mouse monoclonal	BD	347903	FC
Anti-human TCRA/b PE	BW242/412	Mouse monoclonal	Miltenyi Biotec	130-113-531	FC
Anti-human CD4 Alexa Fluor® 594	EPR6855	Rabbit monoclonal	Abcam	ab277931	DSP
Anti-human CD8 Alexa Fluor® 647	C8/144B	Mouse monoclonal	Novus Biologicals	NBP2-34588AF647	DSP
Anti-His	PentaHis	Mouse monoclonal	QIAGEN	34660	ELISA
Anti-mouse IgG (H+L) HRP	–	Goat polyclonal	Jackson ImmunoResearch	115-035-166	ELISA

Anti-Myc	9E10	Mouse monoclonal	Merck Millipore	05-419	WB
Anti-mouse IgG (Fc specific) HRP	–	Goat polyclonal	Sigma-Aldrich	A2554	WB

IHC, Immunohistochemistry; FC, Flow Cytometry; DSP, Digital Spatial Profiling; ELISA, Enzyme-linked immunosorbent assays; WB, Western blot.

Table S2. Rest of reagents

Antigen	Brand	Reference	Application
Neutral buffered formalin	Sigma-Aldrich	HT501128	IHC
DNP-labeled Alu positive control probe II	Ventana, Roche	05272041001	ISH
DAPI	Sigma-Aldrich	D9542-10MG	FC
FcR Blocking Reagent, human	Miltenyi Biotec	130-059-901	FC
LIVE-DEAD Fixable Blue Dead Cell Stain Kit	eBioscience	L34961	FC
LIVE-DEAD Fixable Violet Dead Cell Stain Kit	eBioscience	L34963	FC
Anti-human CD45 - GeoMx Solid Tumor TME Morphology marker	NanoString Technologies	GMX-PRO-MORPH-HST-12	DSP
Anti-human PanCk - GeoMx Solid Tumor TME Morphology marker	NanoString Technologies	GMX-PRO-MORPH-HST-12	DSP
SYTO 13 Nucleic Acid Stain - GeoMx Solid Tumor TME Morphology marker	NanoString Technologies	GMX-PRO-MORPH-HST-12	DSP
GeoMx protein Slide prep kit PCLN	NanoString Technologies	121300312	DSP
GeoMx Immune Cell Profiling Panel	NanoString Technologies	GMX-PROCO-NCT-HICP-12	DSP
GeoMx IO Drug Target Panel	NanoString Technologies	GMX-PROMOD-NCT-HIODT-12	DSP
GeoMx Immune Activation Status Panel	NanoString Technologies	GMX-PROMOD-NCT-HIAS-12	DSP
GeoMx Hyb Code Pack Protein	NanoString Technologies	GMX-PRO-HYB-96	DSP
nCounter Master Kit	NanoString Technologies	NAA-AKIT-012	DSP
Image-iT™ Fixative Solutions	Invitrogen™	FB002	DSP
Citrate Buffer, pH 6.0, 10x, Antigen Retriever	Sigma-Aldrich	C9999	DSP
TintoRetriever Pressure Cooker	Bio SB	7008	DSP
EGFR Fc chimera protein	R&D Systems	344-ER	ELISA
Nunc MaxiSorp™	ThermoFisher Scientific	M9410-1CS	ELISA
Tween®20	Sigma-Aldrich	P1379	ELISA
Tetramethylbenzidine	Sigma-Aldrich	T0440	ELISA
Novex™ WedgeWell™ 10–20% Tris-glycine gels	Invitrogen™	XP10202BOX	WB
Immobilon-PVDF Transfer Membrane	Merck Millipore	IPVH00010	WB
Pierce™ ECL Plus Western Blotting Substrate	ThermoFisher Scientific	32132	WB

QIAamp DNA Blood Mini Kit	QIAGEN	50951104	NGS
FFPE RNA/DNA Purification Plus Kit	Norgen Biotek	54300	NGS
SuperPlex™ Premix	Takara	638543	NGS

IHC, Immunohistochemistry; ISH, *In situ* hybridization; FC, Flow Cytometry; DSP, Digital Spatial Profiling; ELISA, Enzyme-linked immunosorbent assays; WB, Western blot.

Table S3. TCR β statistics

Patient	Sample	Total queries	Total unique clonotypes	Total reads assigned to unique clonotypes	Total unique productive clonotypes	Total reads assigned to unique productive clonotypes	Total unique productive clonotypes with 5-20 aa CDR3	Total reads assigned to unique productive clonotypes with 5-20 aa CDR3	Shannon Index, H	Gini-Simpson Index, D	Pielou's Evenness, J	Clonality score, C
P1	Primary tumor	186,710	3,586	6,684	487	753	215	389	4.702	0.971	0.876	0.124
	Pre-REP	57,164	2,084	20,200	488	12,204	295	12,085	0.772	0.185	0.136	0.864
	REP	131,062	3,171	68,505	720	49,020	355	48,733	0.447	0.106	0.076	0.924
P2	Primary tumor	639,696	13,166	42,613	2,760	6,809	1,532	3,597	5.931	0.977	0.809	0.191
	Pre-REP	320,404	10,625	53,727	2,839	13,776	1,596	11,896	4.237	0.884	0.574	0.426
	REP	462,332	3,096	286,422	1,913	209,019	1,190	209,005	1.529	0.595	0.216	0.784

P1, patient 1; P2, patient 2; REP, rapid expansion protocol; aa, amino acid. Shannon's and Gini-Simpson's indexes, Pielou's Evenness and Clonality scores were calculated from total number of productive clonotypes with CDR3 size between 5-20 aa.